Hindawi Publishing Corporation
Advances in High Energy Physics
Volume 2012, Article ID 504715, 24 pages
doi:10.1155/2012/504715

Review Article

Atmospheric Neutrinos

Takaaki Kajita

Institute for Cosmic Ray Research and Kavli-IPMU, The University of Tokyo, Kashiwa-no-ha 5-1-5, Kashiwa, Chiba 277-8582, Japan

Correspondence should be addressed to Takaaki Kajita, kajita@icrr.u-tokyo.ac.jp

Received 8 July 2012; Accepted 11 September 2012

Academic Editor: Koichiro Nishikawa

Atmospheric neutrinos are produced as decay products in hadronic showers resulting from collisions of cosmic rays with nuclei in the atmosphere. Electron-neutrinos and muon-neutrinos are produced mainly by the decay chain of charged pions to muons to electrons. Atmospheric neutrino experiments observed zenith angle and energy-dependent deficit of muon-neutrino events. It was found that neutrino oscillations between muon-neutrinos and tau-neutrinos explain these data well. This paper discusses atmospheric neutrino experiments and the neutrino oscillation studies with these neutrinos.

1. Introduction

Neutrinos are produced in various places such as in the Sun, the Earth, the atmosphere, and during the core collapse of a massive star. In addition neutrinos are produced in nuclear power plants and with beams of high energy protons. These neutrinos have been studied by various neutrino experiments. One of these experiments is called atmospheric neutrino experiments. These experiments study neutrinos produced by cosmic ray interactions in the atmosphere.

It has been recognized that the small but finite neutrino masses can be understood naturally by the Seesaw mechanism [1–3] by introducing super-heavy neutral particles. Therefore, it is widely understood that the experimental study of neutrino masses and mixing angles are one of the few ways to explore the physics beyond the standard model.

One of the most sensitive methods to observe small neutrino masses is to study neutrino flavor oscillations [4, 5]. If neutrinos have finite masses, each flavor eigenstate (e.g., ν_μ) can be expressed by a combination of mass eigenstates (ν_1, ν_2, and ν_3). The relation

between the mass eigenstates (ν_1, ν_2, and ν_3) and the flavor eigenstates (ν_e, ν_μ, and ν_τ) can be expressed by

$$\begin{pmatrix} \nu_e \\ \nu_\mu \\ \nu_\tau \end{pmatrix} = U \begin{pmatrix} \nu_1 \\ \nu_2 \\ \nu_3 \end{pmatrix}, \tag{1.1}$$

where U is the mixing matrix. The mixing matrix U is expressed by

$$U = \begin{pmatrix} c_{12}c_{13} & s_{12}c_{13} & s_{13}e^{-i\delta} \\ -s_{12}c_{23} - c_{12}s_{23}s_{13}e^{i\delta} & c_{12}c_{23} - s_{12}s_{23}s_{13}e^{i\delta} & s_{23}c_{13} \\ s_{12}s_{23} - c_{12}c_{23}s_{13}e^{i\delta} & -c_{12}s_{23} - s_{12}c_{23}s_{13}e^{i\delta} & c_{23}c_{13} \end{pmatrix}, \tag{1.2}$$

where c_{ij} and s_{ij} represent $\cos\theta_{ij}$ and $\sin\theta_{ij}$, respectively.

For simplicity, let us discuss two flavor neutrino oscillations. The probability for a neutrino produced in a flavor state ν_μ to be observed in a flavor state ν_τ after traveling a distance L through the vacuum is

$$P(\nu_\mu \longrightarrow \nu_\tau) = \sin^2 2\theta_{23} \sin^2 \left(\frac{1.27\Delta m^2_{23}\left(\mathrm{eV}^2\right) L(\mathrm{km})}{E_\nu(\mathrm{GeV})} \right), \tag{1.3}$$

where E_ν is the neutrino energy, θ_{23} is the mixing angle between the flavor eigenstates and the mass eigenstates, and Δm^2_{23} is the mass-squared difference of the neutrino mass eigenstates ($\equiv |m^2_2 - m^2_3|$).

It can be immediately noticed that, in order to study small neutrino masses, one has to study neutrino oscillations with a long neutrino flight length or with a low energy neutrino beam. Atmospheric neutrinos are unique, because they travel very long distances of up to 12,800 km, that is, the diameter of the Earth. The typical energy of these neutrinos is 1 GeV. Therefore, one expects that it should be possible to study neutrino oscillations with atmospheric neutrinos if Δm^2_{23} is $\sim 10^{-4}$ eV^2 or larger.

The above 2-flavor oscillation formula has to be generalized to three-flavor oscillations. In the three-flavor oscillation framework, neutrino oscillations are parametrized by three mixing angles (θ_{12}, θ_{23}, and θ_{13}), three mass squared differences (Δm^2_{12}, Δm^2_{23}, and Δm^2_{13}; among the three Δm^2's, only two are independent), and one CP phase (δ). As we will discuss later θ_{23} and Δm^2_{23} are most relevant to present atmospheric neutrino experiments. θ_{12} and Δm^2_{12} are most relevant to solar and long baseline reactor neutrino experiments. θ_{13} was most recently measured by accelerator-based long baseline and reactor neutrino oscillation experiments.

Due to the hierarchies, $\Delta m^2_{12} \ll \Delta m^2_{23}$ and $\theta_{13} \ll (\theta_{12}, \theta_{23})$, it is approximately correct to assume two-flavor oscillations for analyses of many existing neutrino oscillation data. Therefore, in this paper, first, we discuss the atmospheric neutrino data in terms of two-flavor neutrino oscillations assuming two significantly different Δm^2's. Later we extend our discussions to full three-flavor oscillations.

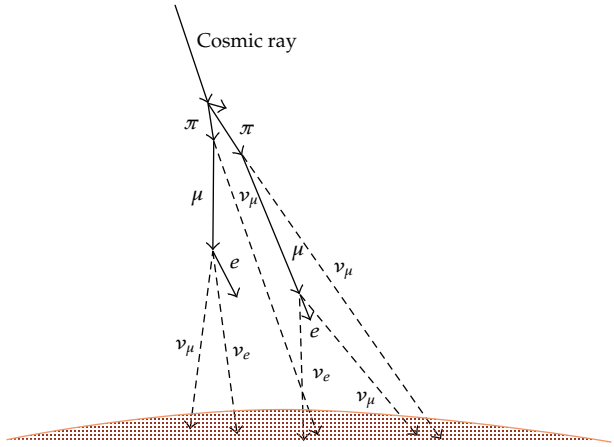

Figure 1: Schematic drawing of the production of atmospheric neutrinos.

2. Atmospheric Neutrino Flux

The study of ν oscillations implies the comparison of the data with theoretical predictions calculated with and without the presence of oscillations.

Cosmic rays are high energy particles arriving at the Earth from the Universe. The cosmic ray flux at the Earth is measured experimentally. In the GeV/nucleon energy region, these cosmic-ray particles are mostly protons, about 5% are Helium nuclei, and a still smaller fraction are heavier nuclei. The energy spectrum of these particles extends to very high energies, although the flux of these particles decreases rapidly with the increasing energy. These particles, once enter into the Earth's atmosphere, interact with the nuclei in the high altitude atmosphere. Typically, in these high energy cosmic ray interactions with the air nuclei, many pions, and less abundantly K mesons, are produced. These mesons decay to other particles: for example, a π^+ decays to a muon (μ^+) and a ν_μ. The produced muon (μ^+) is also unstable and decays to a positron (e^+), a $\overline{\nu}_\mu$ and a ν_e. The charge conjugate decay chain occurs for π^-:

$$\begin{array}{ll} \pi^+ \longrightarrow \mu^+ + \nu_\mu & \pi^- \longrightarrow \mu^- + \overline{\nu}_\mu \\ \quad\quad\downarrow & \quad\quad\downarrow \\ \quad e^+ + \nu_e + \overline{\nu}_\mu & \quad e^- + \overline{\nu}_e + \nu_\mu. \end{array} \tag{2.1}$$

In this manner, neutrinos are produced when a cosmic-ray particle enters into the atmosphere. Smaller contributions come from the kaon decays. Figure 1 shows schematically the production of neutrinos in the atmosphere. These neutrinos are called atmospheric neutrinos.

Equation (2.1) indicates that the fluxes of ν_e, ν_μ's and antineutrinos are strictly related to each other, and in particular that, if all the muons decay, one has

$$\phi(\nu_\mu + \overline{\nu}_\mu) \simeq 2\phi(\nu_e + \overline{\nu}_e), \tag{2.2}$$

where ϕ represents the neutrino flux. In the energy range where some of the muons do not decay before reaching the ground, that is, above a few GeV neutrino energy, $\phi(\nu_\mu + \overline{\nu}_\mu) > \phi(\nu_e + \overline{\nu}_e)$. However, even in this energy range, the flux ratio $\phi(\nu_\mu + \overline{\nu}_\mu)$ over $\phi(\nu_e + \overline{\nu}_e)$ is still

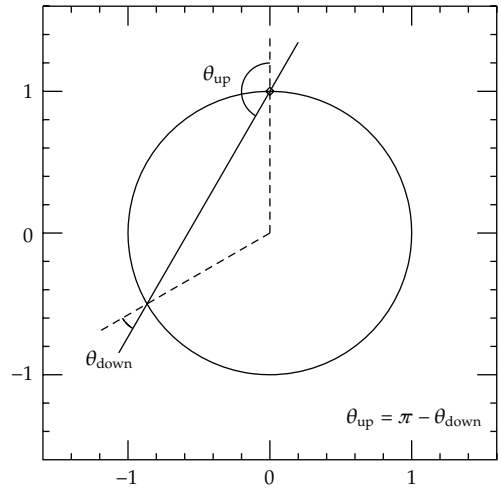

Figure 2: A neutrino trajectory that enters a spherical Earth with zenith angle θ_{down} will exit with a new zenith angle $\theta_{up} = \pi - \theta_{down}$. Assuming that the primary fluxes are equal at the entry and exit points (isotropy) one can deduce the updown symmetry of the fluxes [54].

calculated accurately, because the fraction of muons that decay before reaching the ground can be accurately estimated.

Equation (2.1) also indicates

$$\phi(\nu_\mu) \simeq \phi(\overline{\nu}_\mu), \tag{2.3}$$

because both the π^+ and π^- decay chains produce a ν_μ and a $\overline{\nu}_\mu$. Finally, (2.1) indicates that a ν_e ($\overline{\nu}_e$) is produced by a π^+ (π^-) decay chain. Thus the ν_e over $\overline{\nu}_e$ flux ratio is approximately equal to the π^+ over π^- production ratio. The π^+/π^- production ratio can be estimated by measuring the μ^+/μ^- flux ratio, which is accurately measured. These considerations suggest that, in general, the $\overline{\nu}_\mu$ over ν_μ and $\overline{\nu}_e$ over ν_e flux ratios are also predicted accurately.

Another very robust result of the atmospheric neutrino flux calculation is the prediction that, in the absence of neutrino oscillations, the neutrino fluxes are to a very good approximation updown symmetric for every neutrino type:

$$\phi_{\nu_\alpha}(E, \cos\theta) = \phi_{\nu_\alpha}(E, -\cos\theta), \tag{2.4}$$

where θ is the zenith angle of the neutrino direction. Equation (2.4) can be derived by a geometric argument (see Figure 2), from the assumptions of the isotropy of the cosmic ray flux, and the sphericity of the Earth. However, it should be noted that the updown symmetry is not exact in the neutrino energy range of 1 GeV or less, due to geomagnetic field effects, as discussed later.

The primary cosmic-ray flux decreases rapidly with the energy, approximately $E^{-2.7}$ in the 10 GeV to TeV energy region. Therefore, the calculated neutrino flux rapidly decreases with the increasing energy. Figure 3 shows the calculated energy spectrum of atmospheric neutrinos at the Kamioka and the Soudan-2 sites [6].

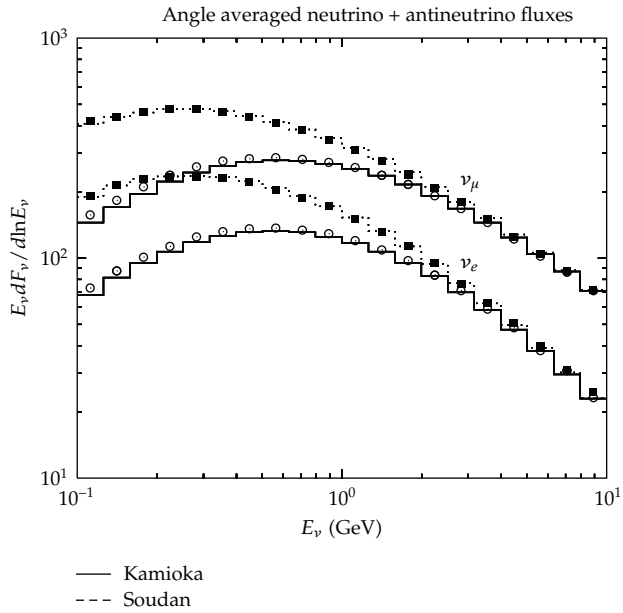

Figure 3: The atmospheric neutrino energy spectrum calculated for the Kamioka and Soudan-2 sites [6]. The $(\nu_\mu + \overline{\nu}_\mu)$ and $(\nu_e + \overline{\nu}_e)$ fluxes are plotted for the three-dimensional (points) and one-dimensional (histograms) calculations. The solid histograms are for the Kamioka site and the dashed histograms are for the Soudan-2 site.

The difficulties and the uncertainties in the calculation of atmospheric neutrino fluxes differ between high and low energies. For low energy neutrinos with energies of about 1 GeV, the primary fluxes of cosmic ray components are relatively well known. On the other hand, the low energy cosmic ray fluxes of less than about 10 GeV are modulated by solar activity and are affected by the geomagnetic field through a rigidity (≡momentum/charge) cutoff. The cutoff is lower near the poles, and therefore the low energy flux is higher for detectors located near the poles than those near the equator. Note that the cosmic ray fluxes in interstellar space are to a very good approximation constant in time and isotropic in direction.

For neutrinos with energy higher than about 100 GeV, primary cosmic rays with energies higher than 1000 GeV are relevant. At these energies, solar activity and the rigidity cutoff do not affect the cosmic rays, but the measurement of the higher energy primary cosmic ray flux is less accurate. In addition, in this energy range, the fraction of K production is a very important factor for the neutrino flux calculation. However, the K production cross-section is not known accurately.

In recent years, the flux calculations have been improved substantially. Results from the most recent work are described below [7, 8]. Figure 4 shows the estimated uncertainty of absolute atmospheric neutrino flux [8]. Practically, the flux calculation can be calibrated by measuring the primary cosmic ray and the secondary muon fluxes. Therefore, in the energy range of 1 to 10 GeV, the estimated uncertainty is less than 10%. Below and above this energy range, the uncertainty gets larger: The uncertainty below 1 GeV is larger due to the limited available data of the secondary muon flux in the GeV energy range at the balloon altitude. Due to the energy loss of the muons in the atmosphere, the muon flux measurement on the ground does not help much in this energy range. In the energy range above 10 GeV,

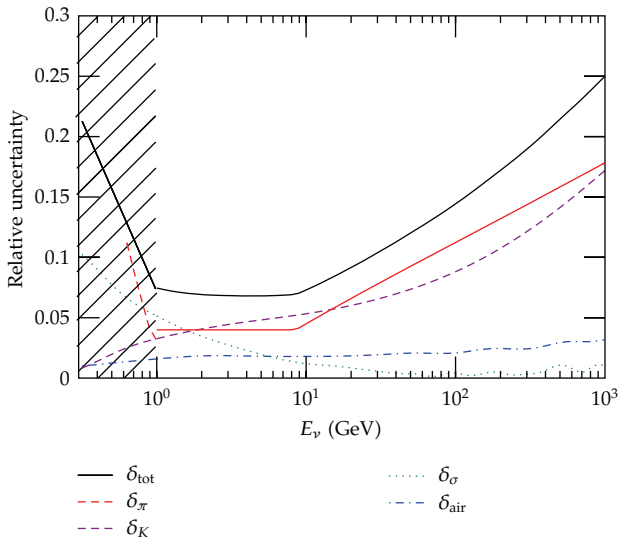

Figure 4: Estimated uncertainty of absolute atmospheric neutrino flux as a function of the neutrinos energy [8]. With the updated flux calculation, the uncertainty below 1 GeV is slightly improved to ~15% at 0.3 GeV [7].

the uncertainty is larger due mainly to the increasing uncertainty of the muon flux and the uncertainty in the K production.

Figure 5 shows the calculated $\nu_\mu + \overline{\nu}_\mu$ over $\nu_e + \overline{\nu}_e$, ν_μ over $\overline{\nu}_\mu$ and ν_e over $\overline{\nu}_e$ flux ratios as a function of the neutrino energy, integrated over solid angle. These ratios are essentially independent of the primary cosmic ray spectrum and the details of the calculation. In the energy region of less than about 10 GeV, most of the neutrinos are produced by the decay chain of pions and the expected uncertainty of the $\nu_\mu + \overline{\nu}_\mu$ over $\nu_e + \overline{\nu}_e$ ratio is about 2 to 3%. In the higher energy region (>10 GeV), the contribution of K decay in the neutrino production is more important. There, the ratio depends more on the K production cross-sections and the uncertainty of the ratio is expected to be larger. We also notice that the ν_μ over $\overline{\nu}_\mu$ flux ratio agrees well among the calculations below a few GeV neutrino energies. Above this energy range, the uncertainties get slightly larger.

Figure 6 shows the zenith angle dependence of the atmospheric neutrino fluxes for several neutrino energies at Kamioka. At low energies, the fluxes of downward-going neutrinos are lower than those of upward-going neutrinos. This is due to the cutoff of primary cosmic rays by the geomagnetic field (rigidity cutoff). For neutrino energies higher than a few GeV, the calculated fluxes are essentially updown symmetric, because the primary particles are more energetic than the rigidity cutoff. The enhancement of the flux near horizon for low energy neutrinos is a feature characteristic of full three-dimensional flux calculations [9, 10]. The 3-dimensional effect is only important below about 1 GeV. However, the horizontal enhancement cannot be seen in the lepton zenith angle distribution, due to the relatively poor angular correlation between neutrinos and leptons below 1 GeV.

The uncertainties in the lepton (not the neutrino) updown and vertical-horizontal ratios can be estimated by comparing the predicted ratios by various flux models by a Monte Carlo simulation. These uncertainties generally depend on the energy and the neutrino flavor. The uncertainty in the updown event ratio is about 1% level in the energy region below 1 GeV

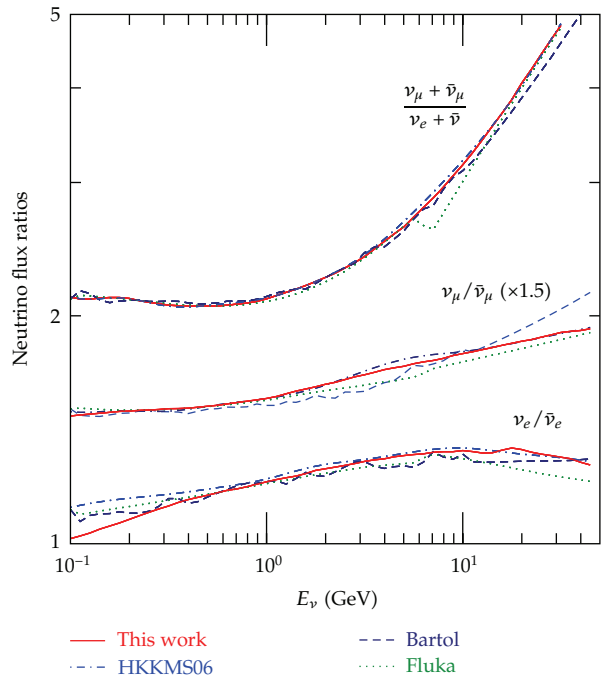

Figure 5: Comparison of the calculated flux ratios for Kamioka by the Bartol group [6], the Fluka group [10], HKKM06 [8] and HKKM11 ("This Work" in the figure) [7].

and is less than 1% above 1 GeV. The main source of the uncertainty in the vertical-horizontal ratio around a GeV is the size of the horizontal enhancement of the flux due to the three-dimensional effect; the uncertainty is estimated to be a few percent or less. In the higher energy region, where upward through-going muons are relevant, the largest source of the uncertainty in the vertical-horizontal ratio is the K production cross-section, and the vertical-horizontal uncertainty is estimated to be 3% [11].

Finally, for the prediction of the observable event rate, one has to include a description of the neutrino cross-sections in the energy range of relevance. For typical atmospheric neutrino experiments, the energy range that needs to be considered is approximately from 0.1 GeV to more than 1 TeV. We refer the details of the neutrino interactions in [12].

3. Brief History

Atmospheric neutrino experiments started in the 1960s. One experiment was carried out in the Kolar Gold Field in India [13]. Another experiment was carried out at the East Rand Proprietary Mine in South Africa [14]. In these experiments, neutrino interactions occurring in the rock surrounding a neutrino detector were measured. Since the experiments were carried out in extremely deep underground (about 8000 meters water equivalent (m.w.e.)), charged particles traversing the detectors almost horizontally were essentially of atmospheric neutrino origin. Also, since it was required that the particle should penetrate through the rock and the detector, most of these neutrino events should have been charged current (CC) ν_μ interactions.

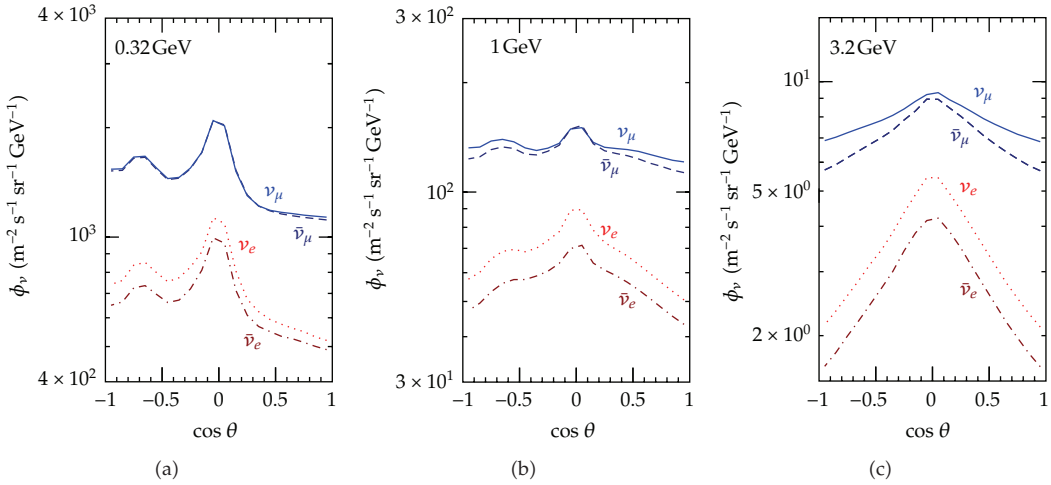

Figure 6: The zenith angle dependence of atmospheric neutrino flux averaged over all azimuthal angles calculated for Kamioka. Here θ is the arrival direction of the neutrino, with $\cos\theta = 1$ (-1) for vertically downward- (upward-) going neutrinos [7].

In the early 1980s, the first massive underground detectors (of the order 1 kton) were constructed, primarily to search for proton decay as predicted by early Grand Unified Theories [15, 16]. The most serious background for proton decay searches was atmospheric neutrino events, at a rate of approximately 10^2 events/kt/yr. Therefore, these experiments were required to study atmospheric neutrino events in order to understand the proton decay background. One of these experiments was Kamiokande. It was a 3-kton water Cherenkov detector. Kamiokande measured the number of single Cherenkov-ring e-like and μ-like events, which were mostly CC ν_e and ν_μ interactions, respectively. In 1988, they found that the number of μ-like events had a significant deficit compared with the Monte Carlo prediction, while the number of e-like events had that in agreement with the prediction within the statistical and systematic errors [17]. As already discussed, the flavor ratio of the atmospheric neutrino flux, $(\nu_\mu + \overline{\nu}_\mu)/(\nu_e + \overline{\nu}_e)$, has been calculated accurately. This can be explained by the deficit of CC ν_μ events. Consistent results were reported from the IMB water Cherenkov experiment in 1991 [18] and from the Soudan-2 experiment in 1997 [19], as well as from the updated analysis of the Kamiokande data in 1992 [20].

Another important hint toward the understanding of the atmospheric neutrino problem was given in the mid 1990s [21]. Zenith angle distributions for multi-GeV fully contained events and partially contained events were studied in Kamiokande. For detectors near the surface of the Earth, the neutrino flight distance, and thus the neutrino oscillation probability, is a function of the zenith angle of the neutrino direction. Vertically downward-going neutrinos travel about 15 km while vertically upward-going neutrinos travel about 12,800 km before interacting in the detector. The Kamiokande data showed that the deficit of μ-like events depended on the zenith angle, and thus on the neutrino flight length. However, due to the relatively poor event statistics, the statistical significance of the updown asymmetry in the Kamiokande data was 2.9 standard deviations, and therefore the data were not conclusive.

In 1996, a much larger detector, Super-Kamiokande, started taking data. Super-Kamiokande (Super-K) is a 50-kton water Cherenkov detector with approximately 11,000 and 1,900 inner and outer detector PMTs. Figure 7 shows the schematic drawing of the

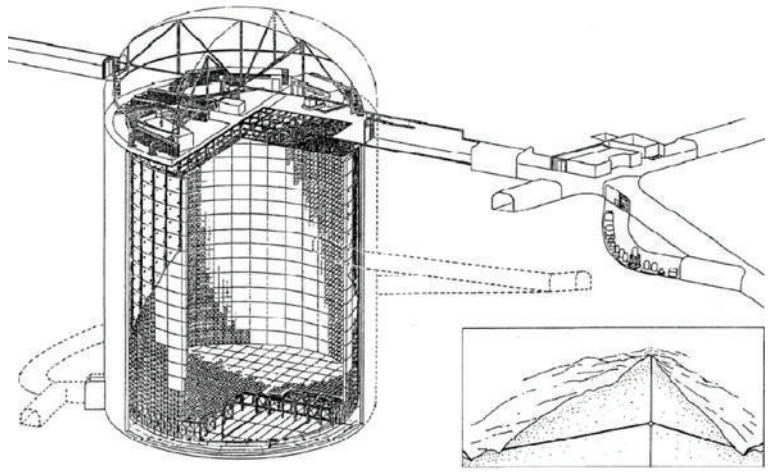

Figure 7: The Super-Kamiokande detector. It is a-50 kton water Cherenkov detector with approximately 11,000 and 1,900 inner and outer detector PMTs. It is located 1-km deep underground.

Super-Kamiokande detector. In 1998, the Super-K experiment, with substantially larger data statistics than those in the previous experiments, concluded that the atmospheric neutrino data gave evidence for neutrinos oscillations [22, 23]. The data clearly showed the deficit of upward-going ν_μ events in the multi-GeV energy range, as well as the smaller μ-like/e-like event ratio than what was expected, the smaller upward-going stopping/through-going muon ratio than what was expected, and the distortion of the zenith angle distribution for the upward through-going muons. In addition, the MACRO [24] and Soudan-2 [25] experiments observed similar distributions with the analyses of upward-going muon data and the contained neutrino data, respectively. Since then, the atmospheric neutrino experiments have been contributing substantially to our understanding of neutrino masses and mixing angles.

4. Present Atmospheric Neutrino Experiments

Atmospheric neutrinos can be detected by underground neutrino detectors. Interactions of low energy neutrinos, around 1 GeV, have all of the final state particles "fully contained (FC)" in the detector. Higher energy charged current ν_μ interactions may result in the muon exiting the detector; these are referred to as "partially contained (PC)." In order to reject background from cosmic-ray particles, as well as to cleanly reconstruct the details of the event, the vertex position of the interaction is typically defined to be within some fiducial volume. In addition, some of the detectors are equipped with outer detectors (also referred to as veto- or antidetectors) to easily identify penetrating particles.

There is a third category of charged current ν_μ events, where the interaction occurs outside the detector, and the muon enters and either passes through the detector or stops in the detector. These are referred to as "upward-going muons" because one generally requires they originate from below the horizon to ensure that a sufficient amount of rock absorbs ordinary cosmic ray muons. The fully contained, partially contained, and upward-going muon event samples have a certain range of parent neutrino energies. As an example, Figure 8 shows the distribution of parent neutrino energies for each category of event samples for the Super-Kamiokande experiment [26]. The energies of atmospheric neutrinos observed

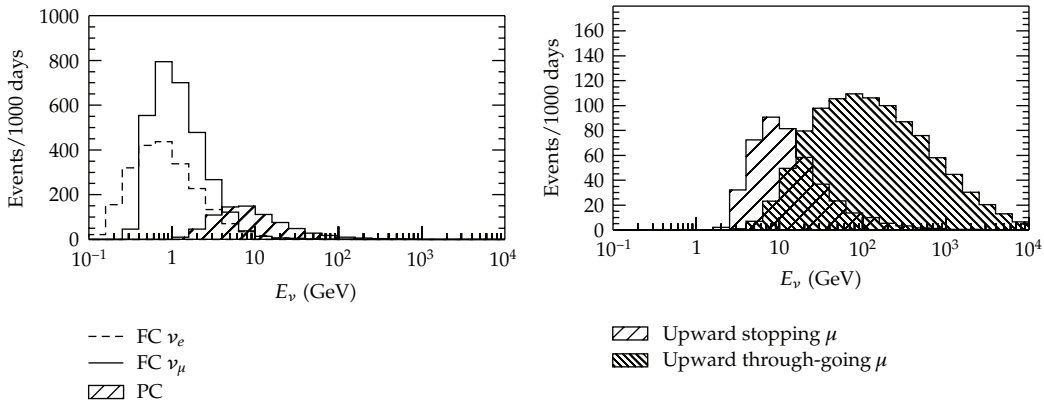

Figure 8: The parent neutrino energy distributions for several different classifications of atmospheric neutrino events for the Super-Kamiokande analysis [26]; for other detectors they will be similar but different depending on detector size, which controls the maximum energy of a fully contained event and the minimum energy of a through-going muon.

in underground detectors range from about 100 MeV to higher than 10 TeV. Depending on the type of experiment, these types of events are studied.

As of this writing, there are four experiments that are presently studying atmospheric neutrinos: Super-K, MINOS, SNO, and IceCube.

SNO was a well-known solar neutrino detector. This experiment was able to measure muons as well, which were generated by high energy atmospheric neutrino interactions in the surrounding rock [27]. Since the SNO detector was located 2 km underground, near-horizontal downward-going muons are neutrino induced. The typical neutrino energy for these muons is 100 GeV. With the currently known Δm^2 value, one can easily estimate that the effect of neutrino oscillation is negligibly small for neutrinos that generate these near-horizontal downward-going muons. Therefore, these muon data can be used to calibrate the calculated atmospheric neutrino flux. The measured downward-going muon flux [27] was 1.22 ± 0.09-times higher than the calculated one by the Bartol group [6]. This result suggests that the absolute flux normalization in the 100 GeV energy range should be improved by future flux calculations.

MINOS is mainly a detector for long baseline neutrino oscillation experiment. However, being located 2070 m.w.e. underground, it can also detect atmospheric neutrinos. It is the first magnetized tracking detector for atmospheric neutrinos. MINOS is able to get information on the track direction, the charge, and the momentum. In [28] the initial results from MINOS on the study of separated atmospheric ν_μ and $\overline{\nu}_\mu$ events were presented. The data were consistent with the standard $\nu_\mu \rightarrow \nu_\tau$ oscillations. The study was updated with significantly more data [29].

IceCube is a neutrino telescope whose main purpose is to study very high energy astrophysical neutrinos. The main background for the search for these astrophysical neutrinos are high energy atmospheric neutrinos. In [30] the atmospheric ν_μ energy spectrum from 100 GeV to 400 TeV was measured. In this energy range, the energy loss of a muon is approximately proportional to $\log(E_\mu)$. Thus the muon and the parent neutrino energy spectra can be estimated. The measured spectrum was consistent with the predictions within the errors.

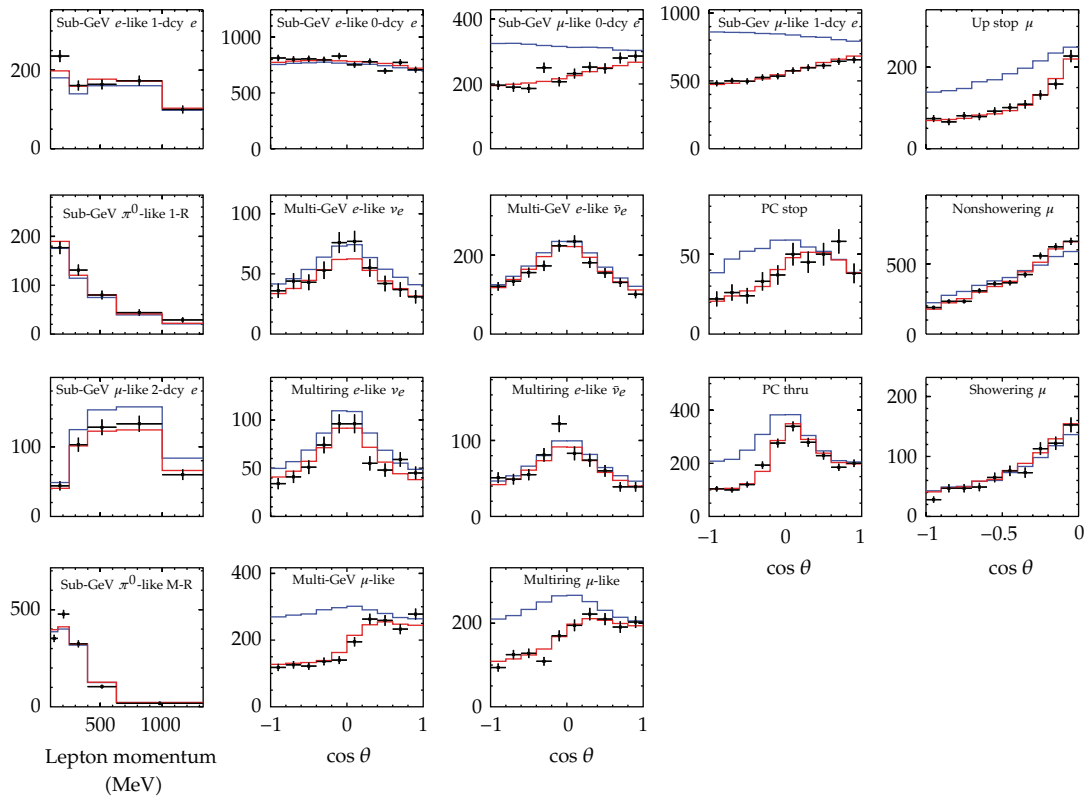

Figure 9: Zenith angle distributions observed in Super-K (240-kton · year exposure), except for 4 panels in the left (which show momentum distributions). The blue histograms show the Monte Carlo prediction without oscillations. The red histograms show the best fit $\nu_\mu \leftrightarrow \nu_\tau$ expectation. Sub-GeV (multi-GeV) events are defined to have the visible energy less (greater) than 1.33 GeV. "PC stop" ("PC through") means partially contained events with at least one particle exiting from the inner detector but stopping in the outer detector.

Recently, IceCube added 8 infill strings to the existing IceCube array (DeepCore). In this volume, lower energy (below 100 GeV) neutrinos can be observed. DeepCore observed the deficit of ν_μ interactions due to neutrino oscillations [31].

These experiments contribute to the studies of atmospheric neutrinos in various ways. However, as far as the neutrino oscillation studies are concerned, the statistics of the atmospheric neutrino events in the relevant energy region are dominated by the data from Super-K. Therefore, hereafter, we mainly discuss the atmospheric neutrino results from Super-K.

Super-K has several phases. Data from Super-K I to IV are used for many physics analyses. The total exposure of the detector for fully contained atmospheric neutrino analysis is 240-kton · yr as of June 2012 [32]. Figure 9 shows the zenith angle distributions for various subsamples from Super-K. Recently Super-K has made a new analysis of enriching the ν_e and $\overline{\nu}_e$ events separately by a maximum likelihood method based on information such as the number of electrons from (pion to) muon decays or the fraction of energy carried by hadrons. The separated distributions for ν_e and $\overline{\nu}_e$ enriched samples are also shown. By fitting the zenith angle distributions (see [26] for the analysis method and the results with less data statistics), the oscillation parameters are accurately measured.

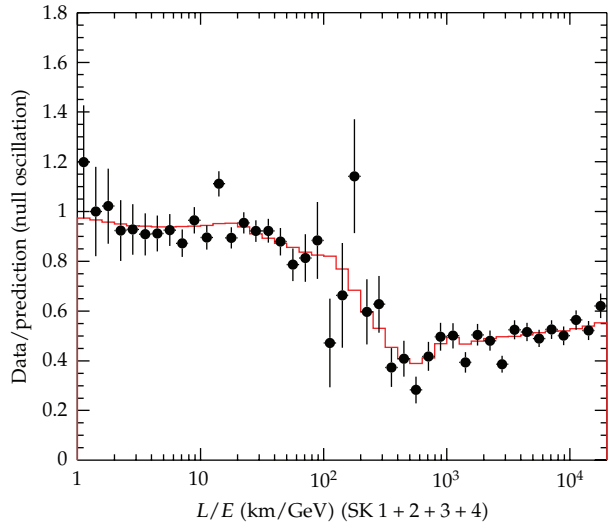

Figure 10: L/E distribution from Super-K (240-kton · year exposure). Data over no-oscillation Monte Carlo prediction are plotted as a function of L/E. Events that satisfy the L/E resolution cut (i.e., $\sigma(L/E) < 70\%$) [33] are used. The red histogram shows the best fit $\nu_\mu \leftrightarrow \nu_\tau$ expectation.

Furthermore, Super-K updated the L/E analysis using only high L/E resolution μ-like and PC events (see [33] for details of the analysis). Figure 10 shows the updated L/E plot from Super-K. One of the initial motivations for the L/E analysis was to test if the ν_μ disappearance probability obeys the sinusoidal function as predicted by neutrino oscillations. This analysis was also used to discriminate the oscillation and the alternative models that fit to the zenith angle distributions rather well. These models included neutrino decay [34, 35] and neutrino decoherence [36, 37] models. The L/E distribution shows a dip around $L/E =$ 500 km/GeV that corresponds to the first oscillation minimum. The distribution is used to compare the oscillation and other hypotheses and to constrain the other hypotheses: the decay and decoherence models are disfavored at 4.0 and 4.8 standard deviations, respectively. Due to the observation of the dip, the allowed region of the oscillation parameters, especially that of Δm^2_{23}, is accurately measured.

4.1. *Flavor Oscillation Analyses*

Neutrino oscillation analyses were carried out using the observed data in various atmospheric neutrino experiments. In these analyses, the treatment of the systematic errors is very important, since, in some cases, the systematic errors have significant effects to the results of the analyses. Therefore, systematic errors are carefully studied and taken into account in the oscillation analyses. In the case of Super-Kamiokande, the number of the systematic error terms in the analyses are more than 100. Some of them are related to the flux, the neutrino interaction, and the detector.

Figure 11 shows the allowed regions of two-flavor $\nu_\mu \leftrightarrow \nu_\tau$ oscillation parameters from the atmospheric neutrino and long baseline neutrino oscillation experiments. We find that the allowed regions overlap well, suggesting further that the standard neutrino oscillation scenario is valid. From this figure, we find that Δm^2_{23} is most accurately measured by the

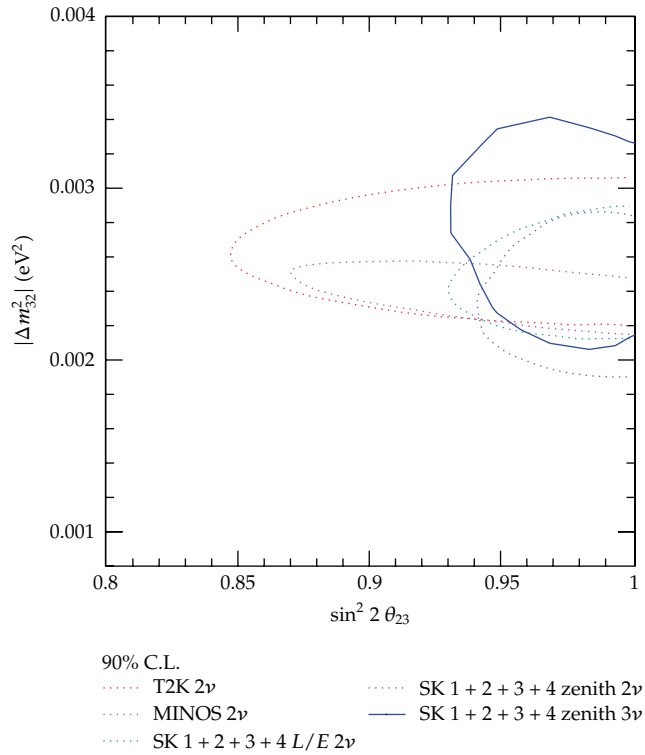

Figure 11: 90% C.L. allowed regions of $\sin^2 2\theta_{23}$ and Δm^2_{23} oscillation parameters from atmospheric neutrino [32] and long baseline [38, 55] neutrino oscillation experiments with $\nu_\mu \leftrightarrow \nu_\tau$ 2-flavor oscillation assumption. For atmospheric neutrinos, results from the zenith angle and L/E analyses are plotted. Also shown is the allowed region on these parameters from the full 3-flavor analysis of the Super-K atmospheric neutrino data. For 3-flavor oscillations, normal mass hierarchy and the best fit $\sin^2\theta_{13}$ are assumed.

MINOS long baseline experiment [38], while the mixing parameter is still measured most accurately by the Super-K atmospheric neutrino experiment. The reason for the possibility to measure $\sin^2 2\theta_{23}$ accurately in atmospheric neutrino experiments can be understood easily: one finds that $1 - \sin^2 2\theta_{23}$ = number of upgoing events/number of down going events in the energy range where the neutrino and the lepton directions have good correlation (i.e., multi-GeV energy range). In addition, the flux is predicted to be updown symmetric to a very good approximation in the multi-GeV energy range. Finally, it should also be noted that $\sin^2 2\theta_{23}$ is consistent with 1.0.

4.2. Tau Appearance

About one CC ν_τ event per kiloton year exposure is expected to occur in an atmospheric neutrino detector for $\nu_\mu \rightarrow \nu_\tau$ oscillations with the present best fit oscillation parameters. The low event rate is due to the soft energy spectrum of the atmospheric neutrino flux and the threshold effect, which requires a ν_τ energy of at least 3.5 GeV to produce a τ lepton. These τ typically decay to hadrons (the branching ratio is 64%) within 1 mm from the vertex point. These events should be upward-going but otherwise similar to energetic NC events. Hence

it is difficult to isolate ν_τ events with the event-by-event bases in the ongoing atmospheric neutrino experiments.

Super-K searched for CC ν_τ events in the multi-GeV FC events. First, it was required that the most energetic ring is e-like, in order to reduce the CC ν_μ background. Then, the candidate ν_τ events were selected by a neural-network method. Several variables of event reconstruction were used as the inputs to these analyses. Then, the zenith angle distribution as a function of the output parameter of the neural network is used to estimate the number of ν_τ events statistically. It is important to notice that the estimation is possible, because both the ν_τ signal and background events have accurately predicted zenith angle distributions. Figure 12 shows the output from the neural-network analysis and the zenith angle distributions from the tau analysis. The best fit number of ν_τ interactions that occurred in the fiducial volume of the detector during the 173-kton $\cdot$ yr exposure was $180.1 \pm 44.3(\text{stat.})^{+17.8}_{-15.2}$ (syst.) [39]. The expected number was $120.2^{+34.2}_{-34.8}$. The observed number of ν_τ interactions was consistent with the $\nu_\mu \rightarrow \nu_\tau$ expectation. As of this writing, the θ_{13} mixing angle has been determined accurately [40–44]. This has a significant impact on the systematic error of the tau appearance, since one of the largest systematic errors in the previous analysis [45] was due to the unknown value of θ_{13}, that is, the unknown contribution of the electron appearance events in the upward-going direction in the tau-like sample. In the most updated analysis [39], ν_τ appearance is required to fit the atmospheric neutrino data with a significance at the 3.8 standard deviation level.

4.3. Flavor Oscillation Analyses

Recent data from the Daya Bay [40], RENO [41], and Double CHOOZ [42] reactor experiments as well as those from the T2K [43] and MINOS [44] long baseline experiments showed that $\sin^2\theta_{13} = 0.0245^{+0.0034}_{-0.0031}$ for normal hierarchy [46]. For inverted hierarchy, the central value is 0.0246 [46]. Although the atmospheric neutrino data are well fit by 2-flavor $\nu_\mu \leftrightarrow \nu_\tau$ oscillations, 3-flavor oscillation effects should be visible at some level. With the observation of nonzero θ_{13}, it is interesting to ask if atmospheric neutrino experiments can determine the mass hierarchy or the CP phase in the neutrino mixing matrix.

Since the 3-flavor oscillations include ν_e's, let us write the oscillation effects as follows:

$$\begin{aligned}\left(\frac{F^{\text{osc}}_{\nu_e}}{F^{0}_{\nu_e}}\right) = {} & \Delta_1(\theta_{13}) \\ & + \Delta_2\left(\Delta m^2_{12}, \theta_{12}\right) \\ & + \Delta_3\left(\theta_{13}, \Delta m^2_{12}, \theta_{12}, \delta\right),\end{aligned} \tag{4.1}$$

where $F^{\text{osc}}_{\nu_e}$ and $F^{0}_{\nu_e}$ are the atmospheric ν_e fluxes with and without oscillations, and Δ_i are the ν_e flux change due to oscillation in matter driven by the parameters listed in the parentheses. Figure 13 shows the oscillation probability ($P(\nu_\mu \rightarrow \nu_e)$) as a function of the neutrino energy (E_ν) and zenith angle ($\cos\Theta_z$). In this plot, normal mass hierarchy is assumed, and the oscillation probability is for neutrinos.

Atmospheric neutrino experiments are sensitive to all the Δ_i's in (4.1). Since the matter enhancement of oscillations is only effective for neutrinos and not for antineutrinos for

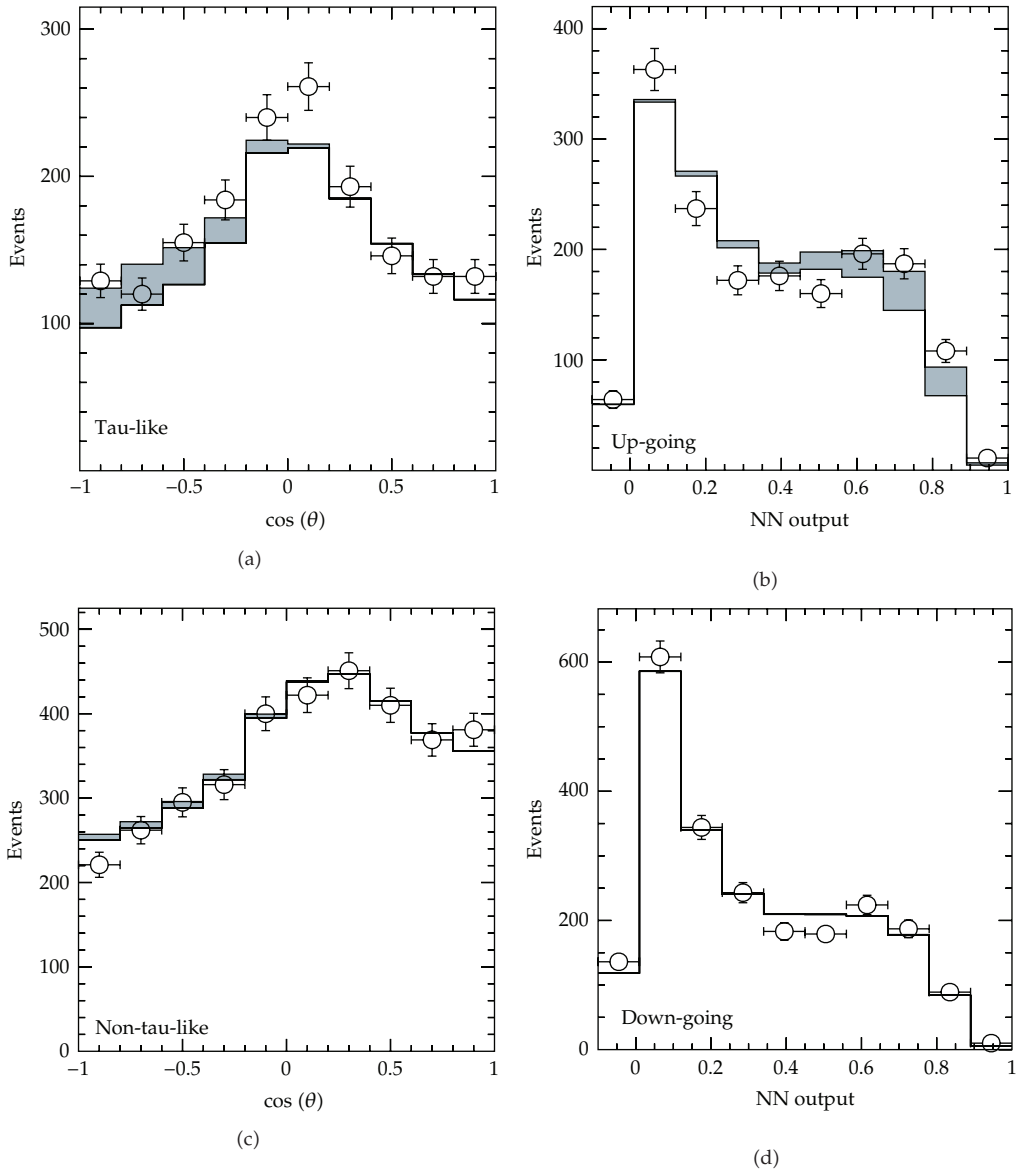

Figure 12: Left: zenith angle distribution for the tau-like and non-tau-like events observed in Super-K I to III (173-kton · yr). The shaded region and solid histogram show the fitted tau neutrino contribution and the non-tau atmospheric neutrino interactions, respectively. Right: fit results showing the output of the neural-network analysis for upward-going and downward-going events. Events near NN output = 1 (0) are most tau-like (non-tau-like).

the normal mass hierarchy, and since there are several features that are different for neutrinos and antineutrino interactions, it might be possible to determine the mass hierarchy with atmospheric neutrino data. The interference term (CP violation term) may also play an important role in atmospheric neutrino oscillations. In fact, some authors (see, e.g., [47]) have indicated the potential importance of the full 3-flavor analysis in atmospheric neutrino experiments, even before the discovery of nonzero θ_{13}.

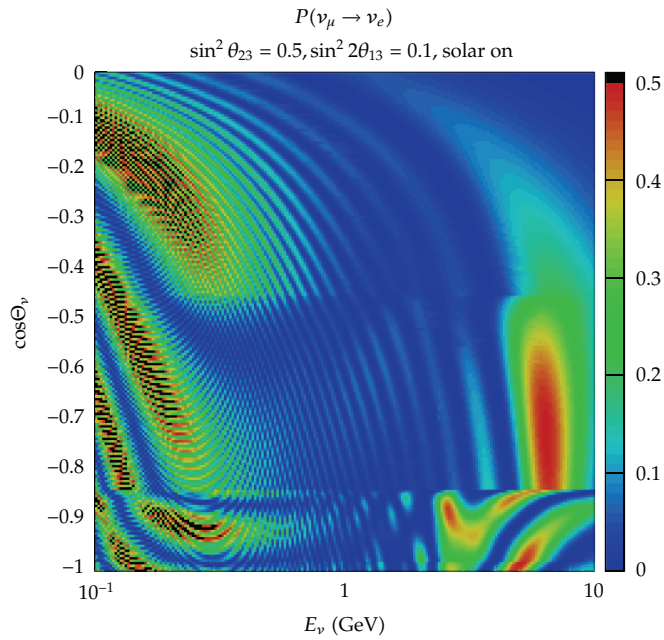

Figure 13: $P(\nu_\mu \to \nu_e)$ is plotted as a function of the neutrino energy (E_ν) and the zenith angle (Θ_z). The oscillation probability is shown by the color. The large oscillation probability in the 5- to 10-GeV energy and for $\cos\Theta_z < 0.5$ is due to θ_{13} with the matter effects. Below about 300 MeV, the oscillation effects due to solar terms with the matter effects are seen. Between these two energy regions, there are effects due to the interference of these two effects (CP phase).

Super-Kamiokande carried out a full 3-flavor analysis [32]. Figure 14 shows the $\chi^2 - \chi^2_{\min}$ distributions as a function of $\sin^2\theta_{13}$ for normal and inverted hierarchy cases. At present, the data are consistent with the reactor and accelerator measurement on $\sin^2\theta_{13}$.

Figure 15 shows the χ^2 distributions as a function of δ_{CP} for normal and inverted hierarchy cases. There is some difference in the χ^2 depending on the mass hierarchies and on δ_{CP}: the χ^2 difference for the best fit δ_{CP} point and the worst fit point is 2.5 for both normal and inverted mass hierarchies. The minimum χ^2 value for the inverted mass hierarchy is smaller than that of the normal mass hierarchy by 1.2. It is clear that the present data cannot determine the mass hierarchy. However, they suggest that the future atmospheric neutrino experiments with much higher statistics or with the ν and $\overline{\nu}$ separation might be able to determine the mass hierarchy.

Figure 16 shows the $\chi^2 - \chi^2_{\min}$ distributions as a function of $\sin^2\theta_{23}$ for normal and inverted hierarchy cases. If θ_{13} is constrained to the present best fit value and the normal hierarchy is assumed, the best fit $\sin^2\theta_{23}$ is less than 0.5. However, in the other cases, the best fit $\sin^2\theta_{23}$ is larger than 0.5. In any case, all the curves suggest that the data are consistent with the maximal mixing, that is, $\sin^2\theta_{23} = 0.5$.

5. Future Directions

Present data from Super-K suggest that future atmospheric neutrino experiments might determine the mass hierarchy and constrain the CP phase. Sensitivity studies have been carried out with different detector technologies.

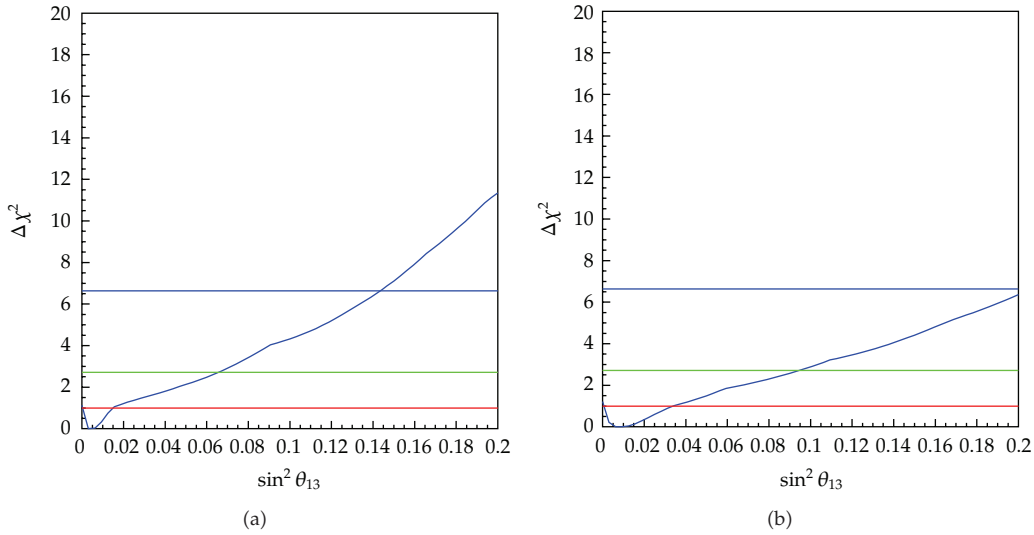

Figure 14: $\chi^2 - \chi^2_{\text{min}}$ distributions as a function of $\sin^2\theta_{13}$ for normal (a) and inverted (b) hierarchies from a full 3-flavor oscillation analysis of the Super-K data. Red, green, and blue lines show 68, 90, and 99% C.L., respectively. The χ^2_{min} is independently calculated for each hierarchy.

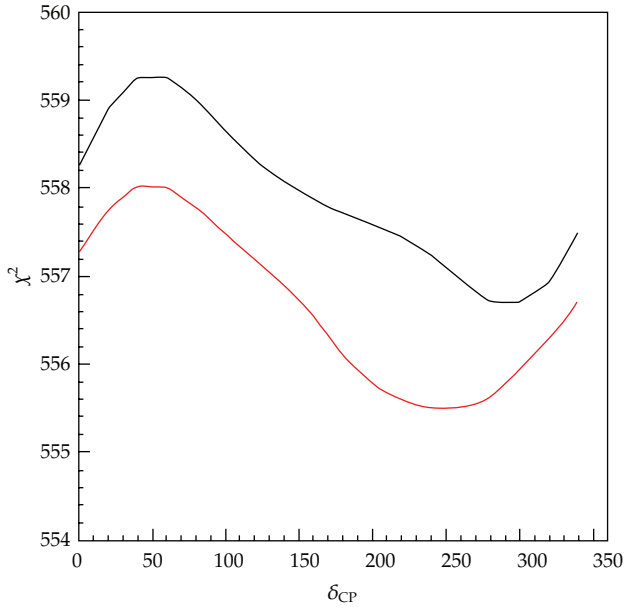

Figure 15: χ^2 distribution as a function of δ_{CP} for normal (black line) and inverted (red line) hierarchies from a full 3-flavor oscillation analysis of the Super-K data.

Figure 17 shows the sensitivity to the mass hierarchy in a water Cherenkov detector (Hyper-Kamiokande) [48]. Hyper-Kamiokande will have 1-Mton total mass and 0.56-Mton fiducial mass. The sensitivity is defined as the χ^2 difference between the normal and inverted mass hierarchies as a function of the detector exposure. Assuming that $\sin^2\theta_{23} = 0.5$ and

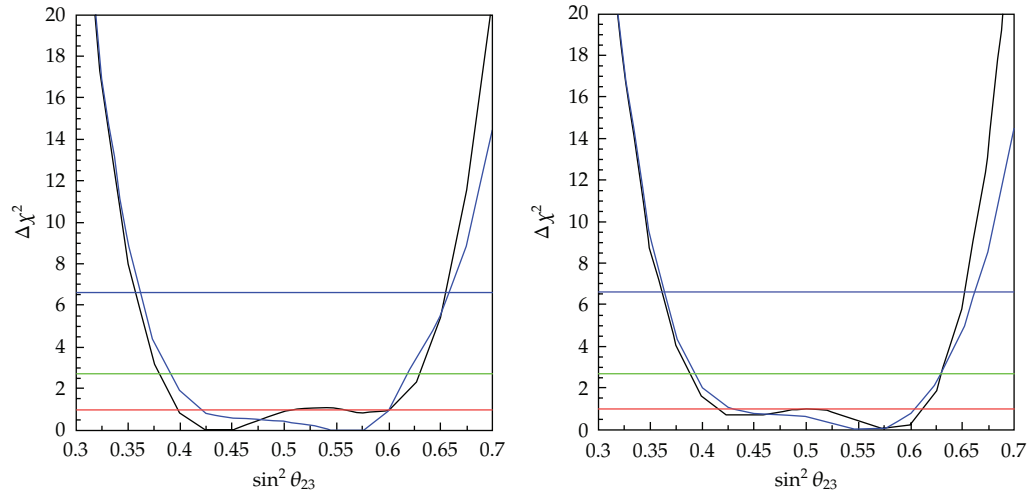

Figure 16: $\chi^2-\chi^2_{\min}$ distributions as a function of $\sin^2\theta_{23}$ for normal (a) and inverted (b) hierarchies from the Super-K full 3-flavor oscillation analysis. Black and blue lines show the χ^2 distributions with and without the constraint of $\sin^2\theta_{13}$.

$\sin^2 2\theta_{13} = 0.1$, the mass hierarchy can be determined at more than the 3-standard deviation level with 5 years of operation for both mass hierarchy cases.

The effects of θ_{13} and mass hierarchy to the ν_μ flux are somewhat smaller. However, if the muon charge is measured, a detector will be sensitive to the mass hierarchy. Figure 18 shows the $P_{\nu_\mu\to\nu_\mu}(\text{NH}) - P_{\nu_\mu\to\nu_\mu}(\text{IH})$ for $\sin^2 2\theta_{13} = 0.1$ and for 2 different zenith angles [49]. One finds the difference for normal and inverted mass hierarchies. The INO project will utilize this feature. The ICAL detector at the INO site will be a 50-kton iron calorimeter detector with 1.5 Tesla magnetic field [50]. Figure 19 shows the schematic view of the ICAL detector, as a typical example of the iron calorimeter detector. Figure 20 shows the expected sensitivity to the mass hierarchy [49]. With the presently known $\sin^2 2\theta_{13}$ it is possible for ICAL to determine the mass hierarchy, although it may take more than 10 years to reach 3-standard deviation level.

Another proposal is to install additional 20 strings to the existing IceCube's DeepCore detector at the South Pole (PINGU) [51, 52]. Due to its huge fiducial mass ($O(10)$ Mton) and a lowered energy threshold compared with IceCube/DeepCore, PINGU will have sensitivity to the mass hierarchy. Figure 21 shows the estimated $(N_\mu^{\text{IH}} - N_\mu^{\text{NH}})/\sqrt{N_\mu^{\text{NH}}}$ for an assumed energy and angular resolutions. Depending on the assumption, it could be possible to determine the mass hierarchy with 5-year data at the 4- to 22-standard deviation level [53].

In addition, it should be pointed out that water Cherenkov detectors are sensitive to the octant of θ_{23} and CP phase due to the possibility of observing subleading effects in the sub-GeV to GeV energy region. Figure 22 shows the expected sensitivity to the octant determination in Hyper-K. Even if $\sin^2 2\theta_{23} = 0.99$, it will be possible to determine the octant of θ_{23} at 90% C.L. for the presently known $\sin^2 2\theta_{13}$.

Future atmospheric neutrino experiments will have some sensitivity to the CP phase as shown in [48]. However, it is also true that the sensitivity is limited compared with the planned accelerator-based long baseline experiments. Probably, atmospheric neutrinos

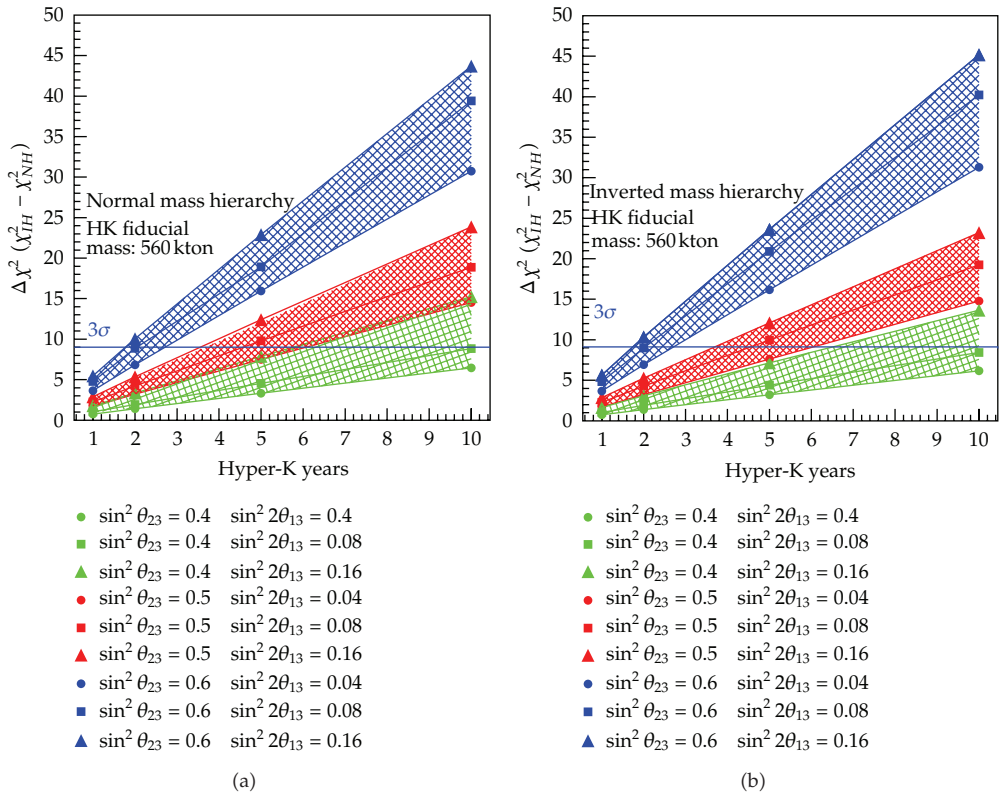

Figure 17: Estimated sensitivity for the determination of mass hierarchy as a function of the Hyper-Kamiokande exposure (years), and as a function of $\sin^2\theta_{23}$ and $\sin^2 2\theta_{13}$. (a) and (b) show the normal and inverted mass hierarchy cases, respectively. Green, red, and blue areas show the estimated $\Delta\chi^2$ ($\equiv\chi^2$ (wrong hierarchy) $-\chi^2$ (correct hierarchy)) for $\sin^2\theta_{23} = 0.4, 0.5$, and 0.6, respectively. The sensitivity weekly depends on the value of $\sin^2 2\theta_{13}$.

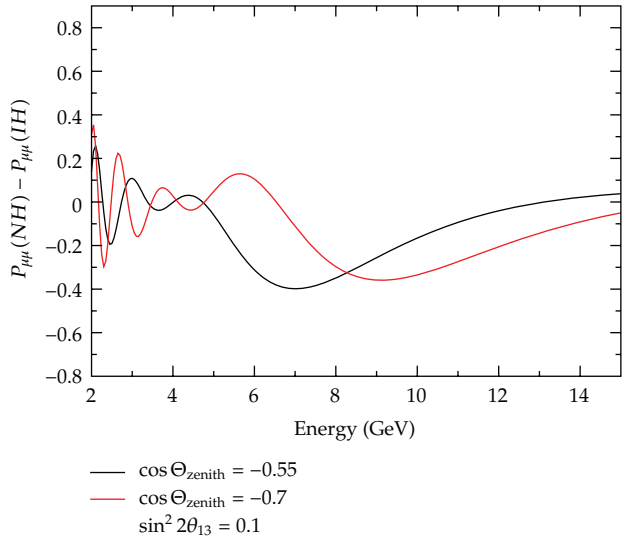

Figure 18: $P_{\nu_\mu\to\nu_\mu}(\mathrm{NH}) - P_{\nu_\mu\to\nu_\mu}(\mathrm{IH})$ for $\sin^2 2\theta_{13} = 0.1$ and for neutrinos propagating through the Earth. Red and black lines show $P_{\nu_\mu\to\nu_\mu}(\mathrm{NH}) - P_{\nu_\mu\to\nu_\mu}(\mathrm{IH})$ for $\cos\Theta_{\mathrm{zenith}} = -0.7$ and -0.55, respectively.

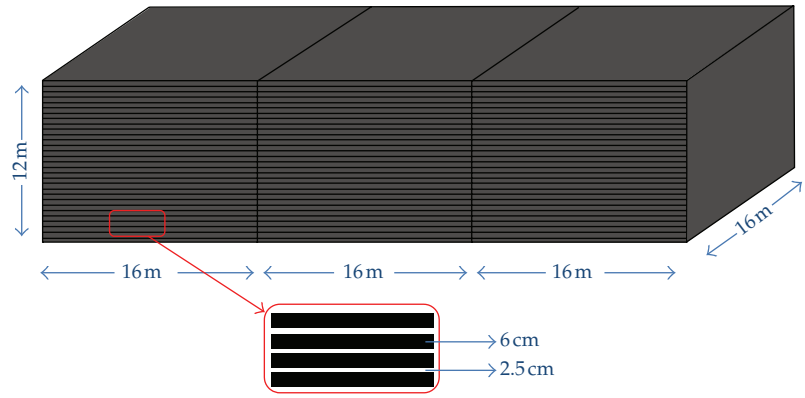

Figure 19: Schematic view of the 50-kton iron calorimeter detector ICAL at the INO site. The detector consists of 3 modules each having 140 layers of magnetized iron plates of 6 cm thickness. The 2.5 cm gaps between the plates house the RPCs.

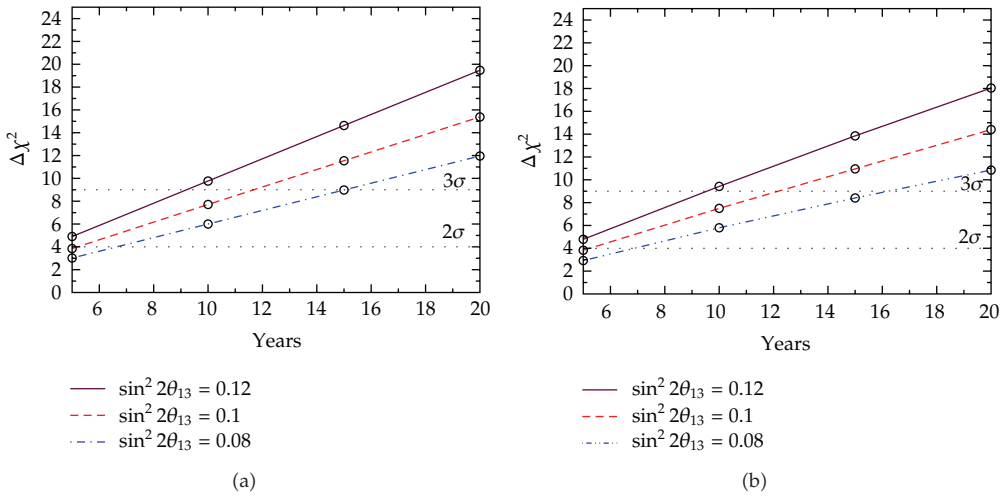

Figure 20: Estimated sensitivity for the mass hierarchy as a function of the ICAL exposure (years), and as a function of $\sin^2 2\theta_{13}$ for normal (a) and inverted (b) hierarchies.

experiments can give independent confirmation of the accelerator results on CP violation. Finally, it should be pointed out that some of the planned long baseline experiments will not have long enough baseline length. Therefore these experiments may not be able to determine the mass hierarchy. If the mass hierarchy is not known, the CP phase cannot be uniquely determined. The determination of the mass hierarchy with future atmospheric neutrino experiments may contribute to eliminate the false CP solution. In this sense, future atmospheric neutrino and long baseline experiments will be complementary.

6. Summary

In this paper, the studies of the atmospheric neutrinos are described. The L/E range in atmospheric neutrinos is very wide, corresponding to the wide neutrino mass range to

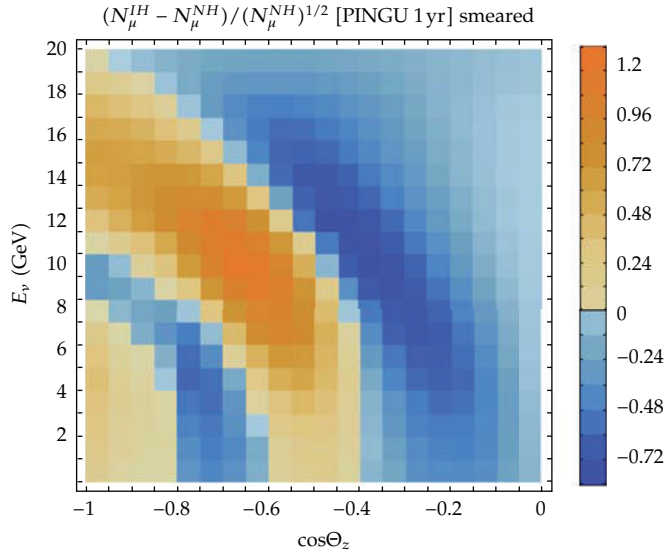

Figure 21: The distribution of $(N_\mu^{\mathrm{IH}} - N_\mu^{\mathrm{NH}})/\sqrt{N_\mu^{\mathrm{NH}}}$ in the (E_ν versus $\cos\Theta_z$) plane. This figure assumes $\sigma_E = 0.3E_\nu$ and $\sigma_\theta = \sqrt{m_p/E_\nu}$.

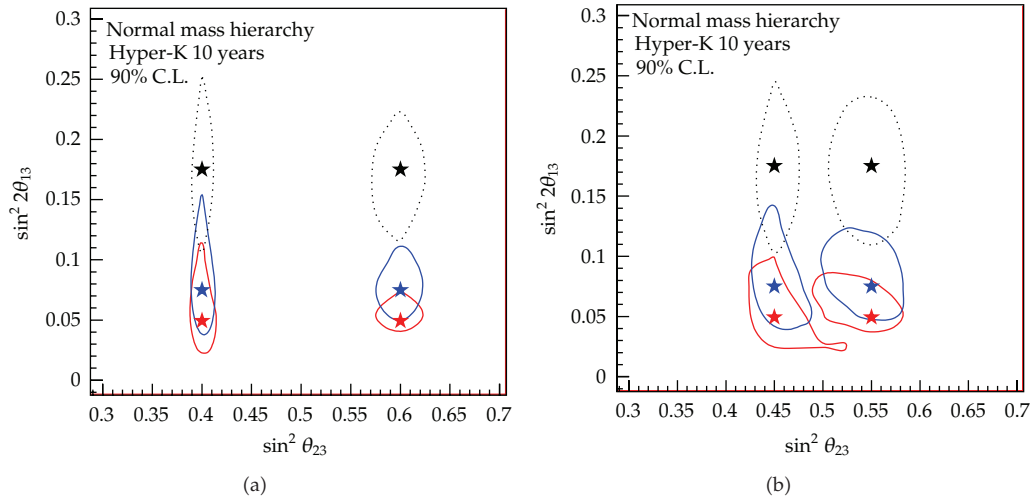

Figure 22: 90% C.L. sensitivity for the determination of octant of θ_{23} as a function of $\sin^2 2\theta_{13}$ after 10 years of the Hyper-Kamiokande operation. (a) shows the case of $\sin^2 2\theta_{23} = 0.96$ ($\sin^2\theta_{23} = 0.4$ or 0.6). (b) shows the case of $\sin^2 2\theta_{23} = 0.99$ ($\sin^2\theta_{23} = 0.45$ or 0.55). Normal mass hierarchy is assumed.

be studied by oscillation experiments. Therefore, in a sense, atmospheric neutrinos were a natural source to discover neutrino oscillations when the neutrino masses were unknown. It took about 10 years from the discovery of the atmospheric neutrino anomaly to the conclusion of neutrino oscillations in 1998. In the subsequent 14 years, the data and the understanding of the neutrino oscillations were improved substantially. These include the confirmation

of $\nu_\mu \leftrightarrow \nu_\tau$ oscillations by accelerator based-long baseline experiments, discovery of solar neutrino oscillations, and the discovery of non-zero $\sin^2\theta_{13}$.

It is widely believed that the discovery of the neutrino masses opened a window to new physics beyond the standard model of particle physics. In particular, large mixing angles seem to be giving us some hint for our deeper understanding in the relation between quarks and leptons. The small but finite neutrino masses could also be the key to the understanding of the baryon and antibaryon asymmetry in the Universe. Largely motivated by these physics, new proposals and ideas for the future neutrino oscillation experiments have been discussed extensively. Atmospheric neutrino experiments are one of them. It is likely that atmospheric neutrino experiments will continue to contribute to the studies of neutrino oscillations.

Acknowledgments

The authors gratefully acknowledge the Members of the Super-Kamiokande Collaboration for useful discussions and information. This work was partly supported by the Japanese Ministry of Education, Culture, Sports, Science and Technology and by the Japan Society for the Promotion of Science.

References

[1] P. Minkowski, "$\mu \to e\gamma$ at a rate of 10^9 muon decays?" *Physics Letters B*, vol. 67, p. 421, 1977.
[2] T. Yanagida, "Horizontal gauge symmetry and masses of neutrinos," in *Proceedings of the Workshop on the Unified Theory and Baryon Number in the Universe*, O. Sawada and A. Sugamoto, Eds., pp. 95–98, 1979, (KEK report 79-18, 1979).
[3] M. Gell-Mann, P. Ramond, and R. Slansky, "Complex spinors and unified theories," in *Supergravity*, P. van Nieuwenhuizen and D. Z. Freedman, Eds., pp. 315–321, North Holland, Amsterdam, 1979.
[4] Z. Maki, M. Nakagawa, and S. Sakata, "Remarks on the unified model of elementary particles," *Progress of Theoretical Physics*, vol. 28, no. 5, pp. 870–880, 1962.
[5] B. Pontecorvo, "Neutrino experiments and the problem of conservation of leptonic charge," *Soviet Physics*, vol. 26, pp. 984–988, 1968.
[6] G. D. Barr, T. K. Gaisser, P. Lipari, S. Robbins, and T. Stanev, "Three-dimensional calculation of atmospheric neutrinos," *Physical Review D*, vol. 70, no. 2, Article ID 023006, 13 pages, 2004.
[7] M. Honda, T. Kajita, K. Kasahara, and S. Midorikawa, "Improvement of low energy atmospheric neutrino flux calculation using the JAM nuclear interaction model," *Physical Review D*, vol. 83, no. 12, Article ID 123001, 2011.
[8] M. Honda, T. Kajita, K. Kasahara, S. Midorikawa, and T. Sanuki, "Calculation of atmospheric neutrino flux using the interaction model calibrated with atmospheric muon data," *Physical Review D*, vol. 75, no. 4, Article ID 043006, 2007.
[9] G. Battistoni, A. Ferrari, P. Lipari, T. Montaruli, P. R. Sala, and T. Rancati, "A three-dimensional calculation of atmospheric neutrino flux," *Astroparticle Physics*, vol. 12, no. 4, pp. 315–333, 2000.
[10] G. Battistoni, A. Ferrari, T. Montaruli, and P. R. Sala, "The FLUKA atmospheric neutrino flux calculation," *Astroparticle Physics*, vol. 19, no. 2, pp. 269–290, 2003.
[11] P. Lipari, "Review of sources of atmospheric neutrinos," *Nuclear Physics B*, vol. 91, no. 1–3, pp. 159–166, 2001.
[12] J. Morfin, J. Nieves, and J. Sobczyk, "Neutrino-nucleus interaction," *Advances in High Energy Physics*. In press.
[13] C. V. Achar, M. G. K. Menon, V. S. Narasimham, P. V. Ramana Murthy, and B. V. Sreekantan, "Detection of muons produced by cosmic ray neutrinos deep underground," *Physics Letters*, vol. 18, no. 2, pp. 196–199, 1965.
[14] F. Reines, M. F. Crouch, T. L. Jenkins, W. R. Kropp, H. S. Gurr, and G. R. Smith, "Evidence for high-energy cosmic ray neutrino interactions," *Physical Review Letters*, vol. 15, no. 9, pp. 429–433, 1965.
[15] J. C. Pati and A. Salam, "Is Baryon number conserved?" *Physical Review Letters*, vol. 31, no. 10, pp. 661–664, 1973.

[16] H. Georgi and S. L. Galshow, "Unity of all elementary particle forces," *Physical Review Letters*, vol. 32, no. 8, pp. 438–441, 1974.
[17] K. S. Hirata, T. Kajita, M. Koshiba et al., "Experimental study of the atmospheric neutrino flux," *Physics Letters B*, vol. 205, no. 2-3, pp. 416–420, 1988.
[18] D. Casper, R. Becker-Szendy, C. B. Bratton et al., "Measurement of atmospheric neutrino composition with IMB-3," *Physical Review Letters*, vol. 66, pp. 2561–2564, 1991.
[19] W. W. M. Allison, G. J. Alner, D. S. Ayres et al., "Measurement of the atmospheric neutrino flavor composition in Soudan-2," *Physics Letters B*, vol. 391, pp. 491–500, 1997.
[20] K. S. Hirata, K. Inoue, T. Ishida et al., "Observation of a small atmospheric v_μ/v_e ratio in Kamiokande," *Physics Letters B*, vol. 280, no. 1-2, pp. 146–152, 1992.
[21] Y. Fukuda, T. Hayakawa, K. Inoue et al., "Atmospheric v_μ/v_e ratio in the multi-GeV energy range," *Physics Letters B*, vol. 335, no. 2, pp. 237–245, 1994.
[22] Y. Fukuda, T. Hayakawa, E. Ichihara et al., "Evidence for oscillation of atmospheric neutrinos," *Physical Review Letters*, vol. 81, no. 8, pp. 1562–1567, 1998.
[23] T. Kajita, "Atmospheric neutrino results from Super-Kamiokande and Kamiokande—evidence for $\nu\mu$ oscillations," *Nuclear Physics B*, vol. 77, no. 1–3, pp. 123–132, 1999.
[24] M. Ambrosio, R. Antolinig, C. Aramo et al., "Measurement of the atmospheric neutrino induced upgoing muon flux using MACRO," *Physics Letters B*, vol. 434, pp. 451–457, 1998.
[25] M. C. Sanchez, W. W. M. Allison, G. J. Alner et al., "Measurement of the L/E distributions of atmospheric neutrinos in Soudan 2 and their interpretation as neutrino oscillations," *Physical Review D*, vol. 68, no. 11, Article ID 113004, 14 pages, 2003.
[26] Y. Ashie, J. Hosaka, K. Ishihara et al., "A measurement of atmospheric neutrino oscillation parameters by Super-Kamiokande I," *Physical Review D*, vol. 71, Article ID 112005, 2005.
[27] B. Aharmim, S. Ahmed, T. Andersen et al., "Measurement of the cosmic ray and neutrino-induced muon flux at the sudbury neutrino observatory," *Physical Review D*, vol. 80, Article ID 012001, 2009.
[28] P. Adamson, T. Alexopoulos, W. Allison et al., "First observations of separated atmospheric v_μ and $\overline{v}_\mu$ events in the MINOS detector," *Physical Review D*, vol. 73, no. 7, Article ID 072002, 2006.
[29] B. Rebel and MINOS Collaboration, "Observation of atmospheric neutrinos and antineutrinos by the MINOS experiment," in *Proceedings of the 25th International Conference on Neutrino Physics and Astrophysics*, Kyoto, Japan, June 2012.
[30] R. Abbasi, Y. Abdou, T. Abu-Zayyad et al., "Measurement of the atmospheric neutrino energy spectrum from 100 GeV to 400 TeV with IceCube," *Physical Review D*, vol. 83, Article ID 012001, 2011.
[31] A. Gross and IceCube Collaboration, "Atmospheric neutrino oscillations with Ice-Cube/DeepCore," in *Proceedings of the 25th International Conference on Neutrino Physics and Astrophysics*, Kyoto, Japan, June 2012.
[32] Y. Itow, "Atmospheric neutrinos—results from running experiments," in *Proceedings of the 25th International Conference on Neutrino Physics and Astrophysics*, Kyoto, Japan, June 2012.
[33] Y. Ashie, J. Hosaka, K. Ishihara et al., "Evidence for an oscillatory signature in atmospheric neutrino oscillation," *Physical Review Letters*, vol. 93, no. 10, Article ID 101801, 6 pages, 2004.
[34] V. D. Barger, J. G. Learned, S. Pakvasa, and T. J. Weiler, "Neutrino decay as an explanation of atmospheric neutrino observations," *Physical Review Letters*, vol. 82, no. 13, pp. 2640–2643, 1999.
[35] V. D. Barger, J. G. Learned, P. Lipari, M. Lusignoli, S. Pakvasa, and T. J. Weiler, "Neutrino decay and atmospheric neutrinos," *Physics Letters B*, vol. 462, no. 1-2, pp. 109–114, 1999.
[36] Y. Grossman and M. P. Worah, "Atmospheric nu/mu deficit from decoherence," http://arxiv.org/abs/hep-ph/9807511.
[37] E. Lisi, A. Marrone, and D. Montanino, "Probing possible decoherence effects in atmospheric neutrino oscillations," *Physical Review Letters*, vol. 85, no. 6, pp. 1166–1169, 2000.
[38] P. Adamson, C. Andreopoulos, R. Armstrong et al., "Measurement of the neutrino mass splitting and flavor mixing by MINOS," *Physical Review Letters*, vol. 106, Article ID 181801, 2011.
[39] K. Abe, Y. Hayato, T. Iida et al., "A measurement of the appearance of atmospheric tau neutrinos by super-kamiokande," http://arxiv.org/abs/1206.0328.
[40] F. P. An, J. Z. Bai, A. B. Balantekin et al., "Observation of electron-antineutrino disappearance at Daya Bay," *Physical Review Letters*, vol. 108, Article ID 171803, 7 pages, 2012.
[41] J. K. Ahn, S. Chebotaryov, J. H. Choi et al., "Observation of reactor electron antineutrino disappearance in the RENO experiment," *Physical Review Letters*, vol. 108, Article ID 191802, 6 pages, 2012.
[42] Y. Abe, C. Aberle, T. Akiri et al., "Indication for the disappearance of reactor electron antineutrinos in the Double Chooz experiment," *Physical Review Letters*, vol. 108, Article ID 131802, 2012.

[43] K. Abe, N. Abgrall, Y. Ajima et al., "Indication of electron neutrino appearance from an accelerator-produced off-axis Muon Neutrino Beam," *Physical Review Letters*, vol. 107, Article ID 041801, 2011.
[44] P. Adamson, D. J. Auty, D. S. Ayres et al., "Improved search for muon-neutrino to electronneutrino oscillations in MINOS," *Physical Review Letters*, vol. 107, Article ID 181802, 2011.
[45] K. Abe, Y. Hayato, T. Iida et al., "A measurement of atmospheric neutrino flux consistent with tau neutrino appearance," *Physical Review Letters*, vol. 97, Article ID 171801, 2006.
[46] G. L. Fogli, E. Lisi, A. Marrone, D. Montanino, A. Palazzo, and A. M. Rotunno, "Global analysis of neutrino masses, mixings and phases: entering the era of leptonic CP violation searches," *Physical Review D*, vol. 86, no. 1, Article ID 013012, 10 pages, 2012.
[47] G. L. Fogli, E. Lisi, A. Marrone, and A. Palazzo, "Global analysis of three-flavor neutrino masses and mixings," *Progress in Particle and Nuclear Physics*, vol. 57, no. 2, pp. 742–795, 2006.
[48] K. Abe, T. Abe, H. Aihara et al., "Letter of intent: the hyper-kamiokande experiment—detector design and physics potential," http://arxiv.org/abs/1109.3262.
[49] S. Choubey, "Future of atmospheric neutrino measurements," in *Proceedings of the 25th International Conference on Neutrino Physics and Astrophysics*, Kyoto, Japan, June 2012.
[50] M. S. Athar, INO Collaboration et al., "India-based Neutrino Observatory: Project Report," Volume I., INO-2006-01.
[51] D. J. Koskinen, "IceCube-DeepCore-PINGU: fundamental neutrino and dark matter physics at the South Pole," *Modern Physics Letters A*, vol. 26, pp. 2899–2915, 2011.
[52] D. R. Grant, "(IceCube/PINGU Collaboration), 'Extending IceCube-DeepCore with PINGU'," in *Proceedings of the 25th International Conference on Neutrino Physics and Astrophysics*, Kyoto, Japan, June 2012.
[53] E. Kh. Akhmedov, S. Razzaque, and A. Yu. Smirnov, "Mass hierarchy, 2-3 mixing and CP-phase with huge atmospheric neutrinodetectors," http://arxiv.org/abs/1205.7071.
[54] T. Kajita and P. Lipari, "Atmospheric neutrinos and neutrino oscillations," *Comptes Rendus Physique*, vol. 6, no. 7, pp. 739–748, 2005.
[55] K. Abe, N. Abgrall, Y. Ajima et al., "First Muon-Neutrino disappearance study with an off-axis beam," *Physical Review D*, vol. 85, Article ID 031103, 2012.